



Universiteit
Leiden
The Netherlands

From the Solo to the Madura Strait: Quaternary geology, vertebrate palaeontology and hominin chronology of eastern Java and submerged Sundaland

Berghuis, H.W.K.

Citation

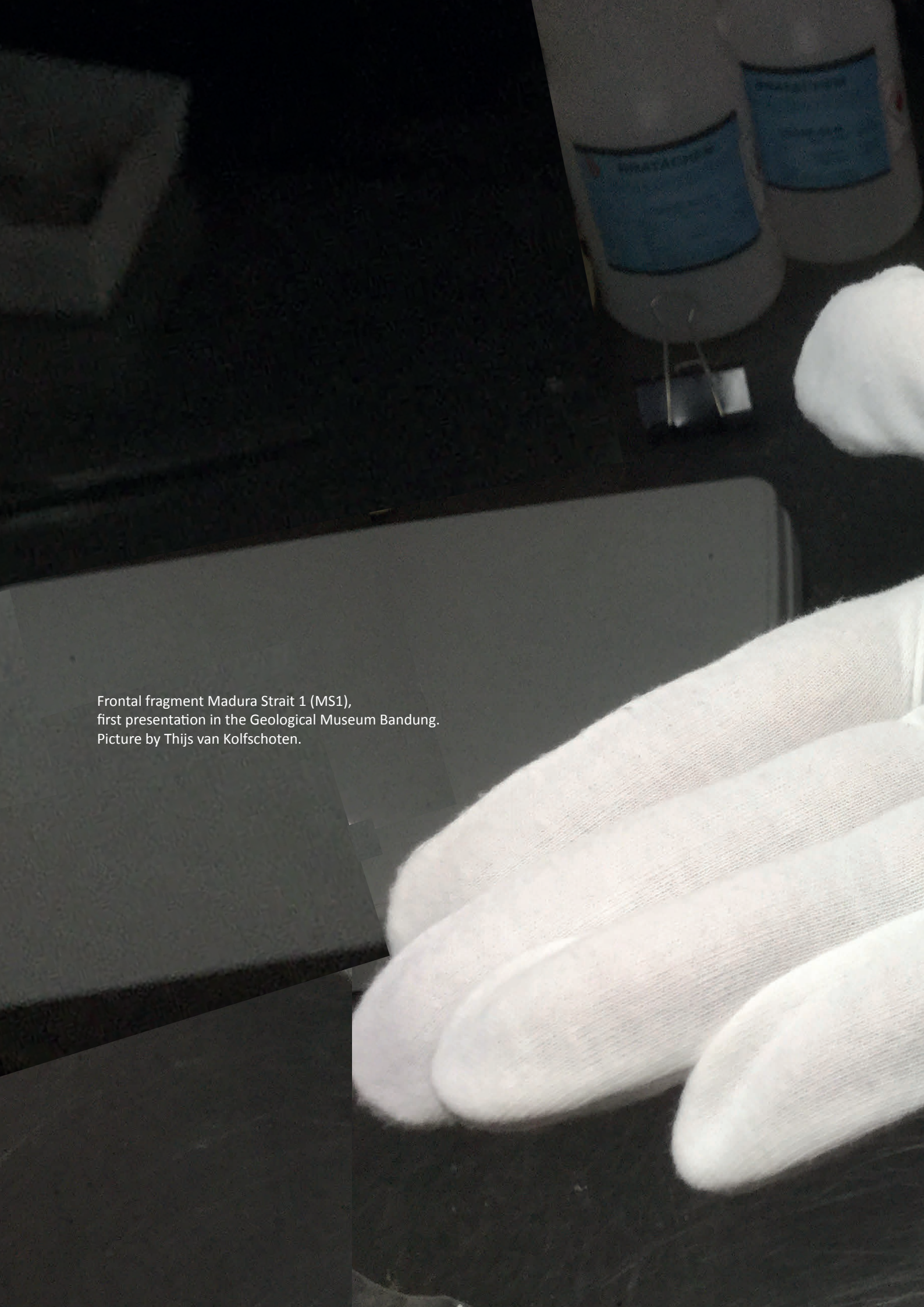
Berghuis, H. W. K. (2026, January 22). *From the Solo to the Madura Strait: Quaternary geology, vertebrate palaeontology and hominin chronology of eastern Java and submerged Sundaland*. Retrieved from <https://hdl.handle.net/1887/4287856>

Version: Publisher's Version

License: [Licence agreement concerning inclusion of doctoral thesis in the Institutional Repository of the University of Leiden](#)

Downloaded from: <https://hdl.handle.net/1887/4287856>

Note: To cite this publication please use the final published version (if applicable).



Frontal fragment Madura Strait 1 (MS1),
first presentation in the Geological Museum Bandung.
Picture by Thijs van Kolfschoten.

Chapter 9

The late Middle Pleistocene *Homo erectus* of the Madura Strait, first hominin fossils from submerged Sundaland



CHAPTER 9

The late Middle Pleistocene *Homo erectus* of the Madura Strait, first hominin fossils from submerged Sundaland

H.W.K. Berghuis, Yousuke Kaifu, Unggul Prasetyo Wibowo, Thijs Van Kolfschoten, Indra Sutisna, Sofwan Noerwidi, Shinatria Adhityatama, Gert Van den Bergh, Eduard Pop, Rusyad Adi Suriyanto, A. Veldkamp, Josephine C.A. Joordens, Iwan Kurniawan

Published in: *Quaternary Environments and Humans* (2025)

Abstract

Eastern Asia yielded a rich fossil record of Pleistocene hominins, ranging from *Homo erectus* and the diminutive island species *Homo florensis* and *Homo luzonensis*, to post-*erectus* grade late archaic *Homo* (including Denisovans), and finally to anatomically modern humans. The Sunda Shelf played an important role in the dispersal and evolution of hominin populations. The shelf has been widely exposed during most of the Pleistocene, forming a landmass known as Sundaland. Today, the area holds the world's largest shelf sea. Thus far, hominin fossils from submerged Sundaland were not available. Here we report on the finding of two hominin cranial fragments from the submerged Sunda Shelf, retrieved during a dredging work in the Madura Strait, off the Java coast. The specimens derive from the sandy fill of a late Middle Pleistocene submerged valley of the Solo River and consist of a frontal fragment and a parietal fragment. Metric and morphological comparisons with Pleistocene skulls from the Asian mainland, Java and Flores point to a relation with the late *Homo erectus* of Java, in particular with the crania from Sambungmacan. The Madura Strait hominins were probably part of an MIS6 population that lived along the Solo, which in this period continued eastward over the exposed shelf area of the Madura Strait. Probably, the large perennial rivers of Sundaland offered good living conditions for *Homo erectus*, in a late Middle Pleistocene climate setting that was relatively dry.

1. Introduction

Hominin diversity and evolutionary complexity in eastern Asia are among the recent foci of paleoanthropological research (Kaifu and Athreya, in press; Bae and Wu, 2024; Liu et al., 2022; Ni et al., 2021). *Homo erectus* appeared in the region during the Early Pleistocene, as shown by fossil remains from China and Java. The late Middle Pleistocene populations of the eastern Asian mainland consist of multiple forms of ‘post-*erectus* grade’ archaic *Homo* including Neanderthals and an enigmatic group called ‘Denisovans’ (Liu and Wu, 2022; Athreya and Hopkins, 2021; Athreya and Wu, 2017; Reich et al., 2010). In contrast, the hominin fossil record of Java suggests a persistence of *H. erectus* throughout the Middle Pleistocene (Baab, 2011; Kaifu et al., 2008; Kidder and Durband, 2004; Schwartz and Tattersall, 2003; Antón, 2003) and possibly into the Late Pleistocene (Rizal et al., 2020).

The Sunda Shelf (Fig. 1A) must have played an important role in regional patterns of hominin dispersal, isolation and evolution (Louys and Turner, 2012; Dennell, 2008). The shelf was probably widely exposed during most of the Early and Middle Pleistocene (Husson et al., 2022, 2020), forming an important habitat for vertebrate species and providing a pathway for *Homo erectus* dispersal to Java. Regional subsidence brought the shelf surface within the range of sea-level fluctuations in the course of the Middle Pleistocene, causing intermittent flooding stages during interglacials (Berghuis et al., 2022; Sarr et al., 2019). The persistence of the Javanese *Homo erectus* lineage throughout the Middle Pleistocene, and possibly into the Late Pleistocene, may relate to this regime of intermittent shelf-submergence, in combination with the remote geographic setting of Java, on the southeastern edge of the Sunda Shelf.

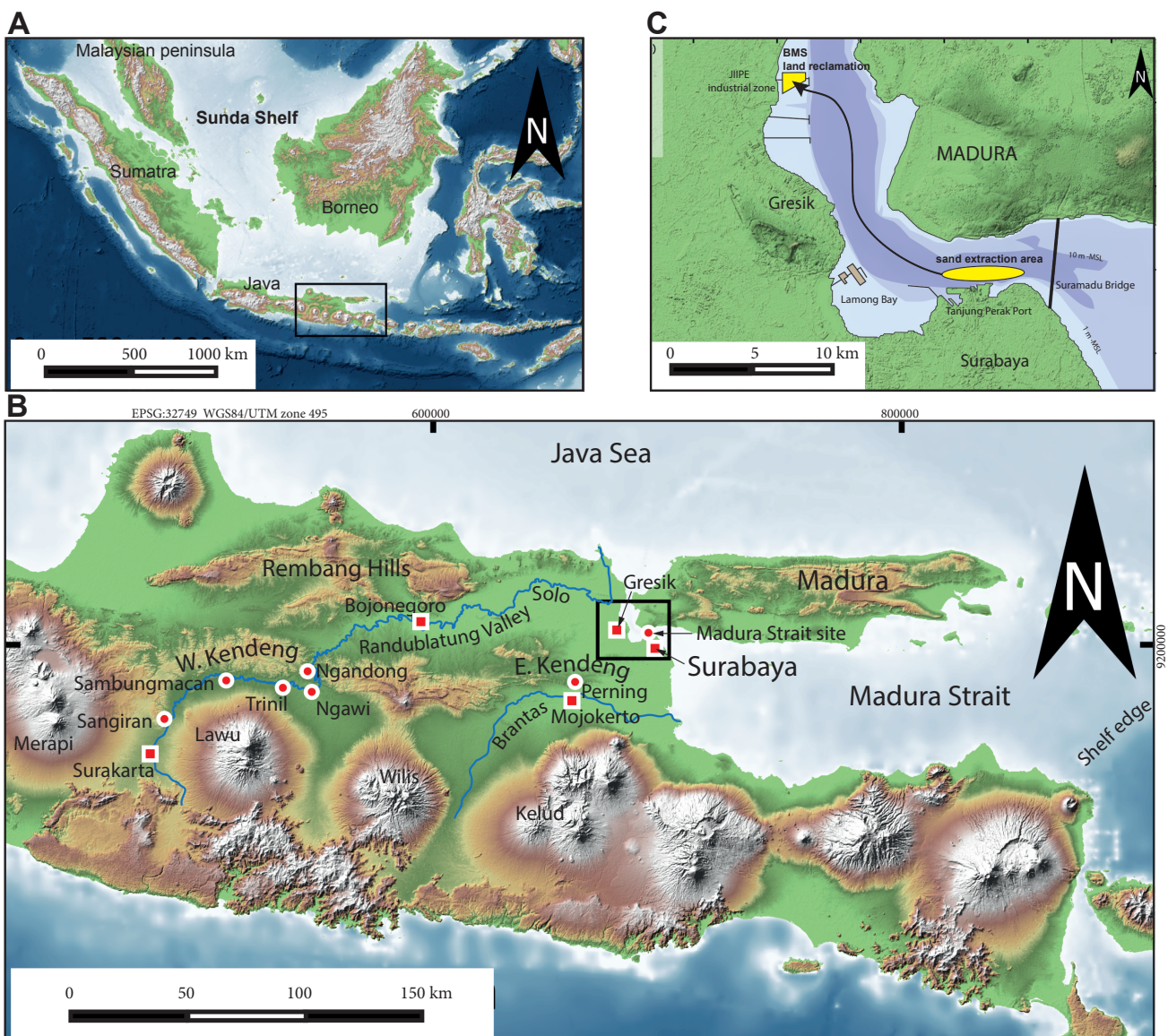


Fig. 1. **A:** The Sunda Shelf of Southeast Asia, with the Indonesian archipelago. Box indicates the position of map B. **B:** Eastern Java, the Madura Strait, the Solo River, Ngandong, Sambungmacan, and other hominin sites. Box indicates the position of map C. **C:** The Madura Strait north of Surabaya, with the sand extraction area and the location of the BMS land-reclamation. Map data: GEBCO and ALOS.

Recent discoveries have brought to light the existence of diminutive Pleistocene hominins on the islands of Luzon and Flores, off the Sunda Shelf, referred to as *Homo luzonensis* and *Homo floresiensis* (Kaifu et al., 2024; Détroit et al., 2019; Brown et al., 2004). Probably, these populations descended from groups of *Homo erectus* who became isolated on these islands and experienced endemic speciation (Kaifu et al., 2024, 2011b; Zanolli et al., 2022).

Meanwhile, genomic studies on extant human populations suggest that there may have been a Late Pleistocene Denisovan population in the Sundaland region, or on Wallacea islands off the Sunda Shelf, prior to the arrival of anatomically modern humans around ~50 Ma (Teixeira et al., 2021; Jacobs et al., 2019; Cooper and Stringer, 2013). Thus far, fossil evidence of this population is lacking.

Clearly, our understanding of hominin dispersal and evolution in this region is hampered by the absence of fossils from the submerged Sunda Shelf. In Berghuis et al. (2025a, 2025b) we presented the first subsea vertebrate-fossil assemblage from this area, retrieved during a dredging work in the Madura Strait, close to the Java coast. The fossils date from the late Middle Pleistocene, an age roughly coinciding with the last recorded presence of *Homo erectus* on Java. Hominin presence at the site was inferred from cut-marks and battered ruminant long bones (Berghuis et al., 2025c). Among the Madura Strait fossils are two hominin skull fragments. In this publication, we present a metric and morphological description of the two specimens and compare them with contemporaneous hominin remains from the region.

2. The Madura Strait site

2.1 Dredging and fossil collecting

In 2014 and 2015, around five million m³ of sand was dredged from the Madura Strait seabed and used for the development of an artificial island along the coast of Gresik, west of Surabaya (Fig. 1B and C). The work was assigned by Berlian Manyar Sejahtera (BMS), a local port company that today uses the island for cargo handling. The work was carried out with a trailing suction hopper dredger. The suction pipe was mounted with a drag head, penetrating and loosening the cemented seabed material. When fully loaded, the vessel sailed to the reclamation site and connected to a floating pipeline to discharge its load.

By April 2015 the artificial island had reached its final surface of ~100 ha (Fig. 2) and was left for dewatering. Upon inspection, the site appeared to be strewn with vertebrate fossils. In the following months, the surface of the site was meticulously searched for fossils, collecting a total of 6,732 specimens. The fossils were stored in the Geological Museum, Bandung.



Fig. 2. The BMS island in the Madura Strait shortly after reclamation, June 2015. View to the east, toward Madura. Courtesy of Pelindo III.

2.2 Geology, age of the subsea site and age of the fossils

The subsea sand-extraction area lies in the port of Surabaya. Over the past decades, the port has been subject to geotechnical studies in relation to port construction works. These data, which include a large number of deep drillings, made it possible to reconstruct the geological setting of the underwater sand extraction site (Berghuis et al.,

2025a). The seabed in this part of the Madura Strait is dominated by a thick unit of firm marine clay, dating from the Late Pliocene to Early Pleistocene. In the central part of the sea strait, this material is incised by tidal currents. Locally, patches of cemented sand and conglomerates have become exposed, reflecting the position of an ancient valley of the Solo. The valley was cut into the clayey subsoil, down to a depth of ca. 50 m –MSL (= local mean sea level) and has a fill of fluvial sandstones with lenses of fine conglomerate, which change upwards into marine clay-sand alternations with fine shell debris (Fig. 3). The sandy fill follows the standard sequence of transgressively-filled valleys (Bowen and Weimer, 2003). The basal conglomerate forms a fluvial lag that relates to the incision of the valley, during a stage of falling sea level. The overlying sandstones represent fluvial back-filling during the subsequent stage of rising sea level. Occasional conglomerate interbeds reflect a stacking of flow channels during this aggradation stage. The upward change to marine sandstones and clays indicates that eventually the valley drowned and changed into an estuary. Sand excavation proceeded down to a depth of 32 m –MSL, cutting through the marine top of the valley fill and several meters into the underlying fluvial sandstones with occasional conglomerate beds.

On the BMS reclamation site, the facies of the excavated material can be recognized in blocks of uncrushed sediment. These consist of laminated marine sandstone and clay with fine shell debris, or cross-bedded fluvial sandstones and conglomerates. The latter two contain dispersed, fragmented skeletal remains. Two fluvial sandstones samples, collected from the reclamation site, have been OSL-dated. One sample derives from a block of uncrushed fluvial sandstone with adhered vertebrate fossils. The second sample was taken from the sandstone fill of the neural canal of a cervid vertebra. The found OSL-ages, of 162 ± 31 and 119 ± 27 ka, link fluvial backfilling of the paleovalley to the lowstand of MIS6 and the subsequent transgression in the run-up to MIS5 (Berghuis et al., 2025a). Valley incision probably relates to the preceding stage of falling sea-level, prior to peak lowstand conditions of MIS6.

On the reclamation site, occasional blocks can be observed of a marine conglomerate, consisting of rounded gravel and broken shells in a calcite-cemented matrix of volcanic sand and shell debris. Remarkably, this material is exceptionally rich in fragmented skeletal remains. On the core logs of the deep drillings, this marine conglomerate forms a ca. 1 m thick interbed at the boundary between the fluvial and marine valley fill. The material is regarded as a tidal lag deposit, reflecting increased energy conditions during the early drowning stage of the river mouth. The gravel and fossils were probably reworked from the underlying fluvial sediment.

The on-land vertebrate fossil sites of Java often bear evidence of multiple cycles of fluvial erosion and sedimentation, resulting in complex and often mixed-age fossil assemblages, either as a result of reworking or uncontrolled fossil collecting (Pop et al., 2023a; Hilgen et al., 2023; Berghuis et al., 2023, 2022, 2021). However, these sites represent upstream fluvial settings, which have been subject to variable and often short-duration fluvial responses to sea-level fluctuations, tectonism or volcanism. It is reasonable to assume that the Sundaland plains offered more stable conditions, with large lowland rivers that responded primarily to sea-level fluctuations.

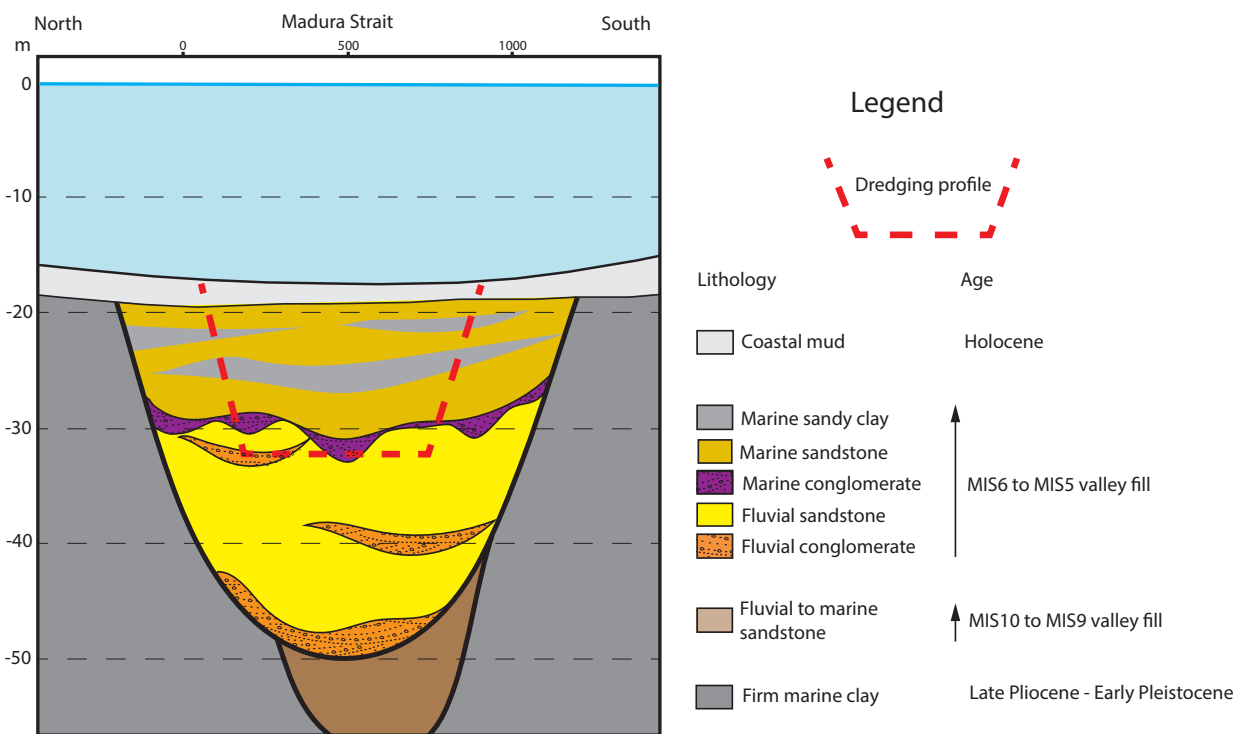


Fig. 3. Schematic cross-section of the Madura Strait paleovalley north of Surabaya and depth profile of the dredging work. Cross-section is based on deep drilling data of the Suramadu Bridge. For details, see Berghuis et al. (2025a and c).

Assuming that the MIS6 to MIS5 stage of rising sea-level offered stable conditions of fluvial backfilling, the skeletal remains in the fluvial sediment may be regarded as a homogeneous fauna, with an age that is contemporary to the age of burial. The age may be narrowed to 146 – 131 ka, which is the overlapping interval of the two OSL-ages and their margins. This ‘most likely age range’ fits well with the proposed model of valley-aggradation and valley drowning, as it overlaps with the stage of rising sea-level between MIS6 and MIS5 (Berghuis et al., 2025c). Concentration of fossils in the marine lag is associated with the subsequent drowning of the valley, which must have slightly predated peak MIS5e highstand conditions of 123 ka. The overlying marine sandstones and clays may be tied to MIS5e.

2.3 The fossil fauna

The vertebrate assemblage from the Madura Strait site covers 36 species, divided over 11 orders (Berghuis et al., 2025b). The assemblage is dominated by remains of large bovids *Bos palaeosondaicus* and *Bubalus palaeokerabau*, as well as the elephantoids *Stegodon trigonocephalus* and *Elephas* sp. This herbivore-dominated community points to open vegetation conditions and a relatively dry climate, which is in line with the Middle Pleistocene pollen record of Java (Sémah et al., 2010; Van der Kaars and Dam, 1995). This was probably also the case for the greater Sundaland region, especially during glacial stages (McGrath et al., 2023; Louys and Roberts, 2020; Louys and Meijaard, 2010; Bird et al., 2005). The fossil fauna roughly overlaps with the contemporaneous assemblage of Ngandong (Java). Nevertheless, there are some noteworthy differences. Among the terrestrial herbivores of the Madura Strait, the presence of *Duboisia santeng*, *Epileptobos groeneveldtii* and *Axis lydekkeri* is interesting. These species are unknown from Ngandong and were previously regarded to have gone extinct on Java in the second half of the Middle Pleistocene. Their presence in the Madura Strait indicates that the species persisted on the emerged lowland plains. Another difference is that the Madura Strait assemblage is richer in fluvial reptiles and estuarine and fluvial fish, which marks the difference between a lowland setting (Madura Strait) and an upland setting (Ngandong). Fossils of estuarine species probably derive from the top of valley fill, which is associated with peak MIS5e highstand conditions.

3. Material and methods

We here report two hominin cranial fragments from the Madura Strait fossil assemblage. Madura Strait 1 (MS1; catalogue no. SBY7120), a right frontal bone fragment, was picked up from the reclamation site in September 2018 by H.B. and was recognized as a hominin frontal fragment at the spot (find coordinates: 7°05'06.82"S / 112°38'42.63"E). Madura Strait 2 (MS2; catalogue no. SBY7211), a parietal fragment, was picked up from the reclamation site in 2015 by H.B., but was only recognized as a hominin skull fragment during later registration work at the Geological Museum, Bandung. Its exact findspot on the reclamation site is unknown.

High-resolution CT imagery of MS1 was obtained using the microfocal X-ray CT system TX225-ACTIS (Tesco Co.), at The University Museum, University of Tokyo, with the following parameters: 130 kV, 0.24 mA, and 35.18524 microns voxel size. At present, MS2 has not been CT-scanned.

Metric data of MS1 and MS2 were taken with a digital calliper and, for the case of MS1, CT data. The supraorbital torus thickness (SOTT) is the superoinferior thickness measured at the free anterior margin of the brow ridge. The thicknesses were measured at mid-orbit (SOTT mid) and at the lateral corner of the orbit (SOTT lat). Supraorbital torus breadth (SOTB) is the maximum transverse breadth of the frontal across the supraorbital tori. Postorbital breadth (POBB) is the least transverse breadth of the frontal squama measured behind the supraorbital torus, in the concavity of the postorbital constriction. One-sided postorbital constriction (POC 1-sided) is a half of the difference between SOTB and POBB.

The comparative materials are the following *Homo erectus* and post-*erectus* grade archaic *Homo* fossils from Java and other insular (Flores) and continental (China and India) parts of eastern Asia:

The late Early Pleistocene *H. erectus* from Java

This group is represented by the fossils from Sangiran and Trinil. The material may be further divided into two chronological subgroups, referred to as archaic and typical *H. erectus* by Widianto and Noerwidi (2023) or as the Sangiran Lower and Upper paleodememes by Kaifu and Athreya (in press). Referring to the most recent chronologies of Matsu'ura et al. (2020) and Hilgen et al. (2023), the paleodememes date to ~1.1 - 0.9 Ma and 0.9 – 0.773 Ma respectively. The most relevant comparative crania belong to the younger subgroup.

The late Middle Pleistocene *H. erectus* from Java

This group is represented by fossils from Ngandong, Sambungmacan and Ngawi. The material may be referred to as the late Javanese *Homo erectus* (Antón, 2003), or as progressive *Homo erectus* (Widianto and Noerwidi, 2023), or as the Ngandong/Sambungmacan/Ngawi paleodeme (Kaifu and Athreya, in press). The fossils are dominated by cranial remains, found along the middle reach of the Solo. The fossils from Ngandong derive from a fluvial terrace that was dated to 140-92 ka (Rizal et al., 2020), which implies that they may date from the early Late Pleistocene. This, how-

ever, is not very likely. The fossil fauna from Ngandong is the last representant of the Middle Pleistocene grassland or open-woodland vertebrate community of Java and most likely pre-dates the forested conditions of MIS5e (Sondaar, 1984). It is therefore plausible to project the Ngandong skulls in the early part of the age range, roughly between 140 and 130 ka, which links the population to the penultimate glacial period of MIS6. The fossils from Sambungmacan and Ngawi are regarded as roughly contemporaneous with or slightly older than those from Ngandong, based on cranial morphology and limited stratigraphic data (Kaifu et al., 2015; Baba et al., 2003; Antón, 2003).

***Homo floresiensis* from Flores**

This group is represented by early Middle Pleistocene material from Mata Menge and Late Pleistocene material from Liang Bua. From the latter site a relevant comparative skull is available (Kaifu et al., 2011b; Brown et al., 2004).

The early Middle Pleistocene *H. erectus* from northern China

This group is referred to as the Zhoukoudian paleodeme by Howell (1999) and Kaifu and Athreya (in press) and includes fossils from Zhoukoudian Locality 1, and possibly Nanjing (Tangshan) and several other sites (Xing et al., 2018).

The mid-Middle Pleistocene late archaic *Homo* from Hexian, northern China

The skull from this site has a unique morphology (Liu et al., 2017; Kaifu, 2017). Its taxonomic placement is controversial (Kaifu and Athreya, in press), which is why the skull is treated separately within the comparative sample of this study.

The late Middle Pleistocene to early Late Pleistocene late archaic *Homo* from northern and central China

This group, which includes the skulls from Hualongdong, Xuchang, Dali, Jinniushan, and Harbin, may or may not represent multiple species, but we do not separate them because of ongoing controversy (Ni et al., 2021; Liu et al., 2022; Bae and Wu, 2024; Kaifu and Athreya, in press).

The late Middle Pleistocene archaic *Homo* from southern China and India

This group consists of the skulls from Maba (Wu et al., 2011) and Narmada (Cameron et al., 2004). They differ from the northern Chinese archaic *Homo* by their facial morphology (Kaifu and Athreya, in press; Howell, 1999).

4. Results

4.1 Descriptions

4.1.1 Madura Strait 1

Madura Strait 1 (Fig. 4) is a frontal fragment, which measures 45 mm mediolaterally and 33 mm anteroposteriorly. It preserves the lateral two-thirds of the dextral supraorbital torus, the supratoral plane, and the basal part of the frontal squama. The specimen is heavily mineralized, exhibits a dark color, and is free from taphonomic distortion. The outer bone surface is well-preserved, except for some minor erosion pits. The inner bone surfaces, i.e. the orbital roof and endocranial surface, are substantially damaged so that much of the cortical bone was lost. Small patches of matrix, almost indistinguishable from the bone in our micro-CT scan, sporadically remain on the bone surfaces. The original orientation of MS1 is difficult to determine, as the orientation of this part of the supraorbital region varies in the comparative sample. In Fig. 4A and B, MS1 is oriented with the axis of the torus placed slightly diagonally and in Fig. 4C more horizontally.

In the anterior view, the supraorbital torus of MS1 is relatively straight. A weak bulge on the supratoral plane forms the lateral end of the glabellar part of the supraorbital torus (or superciliary arch) (Fig. 4C). The medial aspect the supraorbital margin is accentuated by a gentle, but transversely wide bulge, which probably is a form of the supraorbital process. Medial to this supraorbital process, the superior orbital margin curves gently upward, indicating the presence of a shallow supraorbital notch in the missing medial portion of the frontal. Lateral to this supraorbital process, the vertical thickness of the supraorbital torus remains similar throughout, with no marked lateral thickening at its lateral junction with the temporal line.

Viewed superiorly, the anterior orbital margin is gently curved with no marked development of the supraorbital fissure (frontal incisura) between the glabellar and lateral parts of the supraorbital torus. Postorbital constriction is very weak behind the small zygomatic process. Behind the supratoral plane, the frontal squama is weakly inclined posteriorly, forming a gentle angle with the supratoral plane. Posterior to the lateral part of the supratoral plane and medial to the temporal line that forms the border between the superior and lateral parts of the frontal squama, the antero-lateral part of the frontal squama is weakly concave. The CT scan (Fig. 4D) indicates that the preserved lateral portion of the supraorbital torus is dense with no lateral development of the frontal sinus.

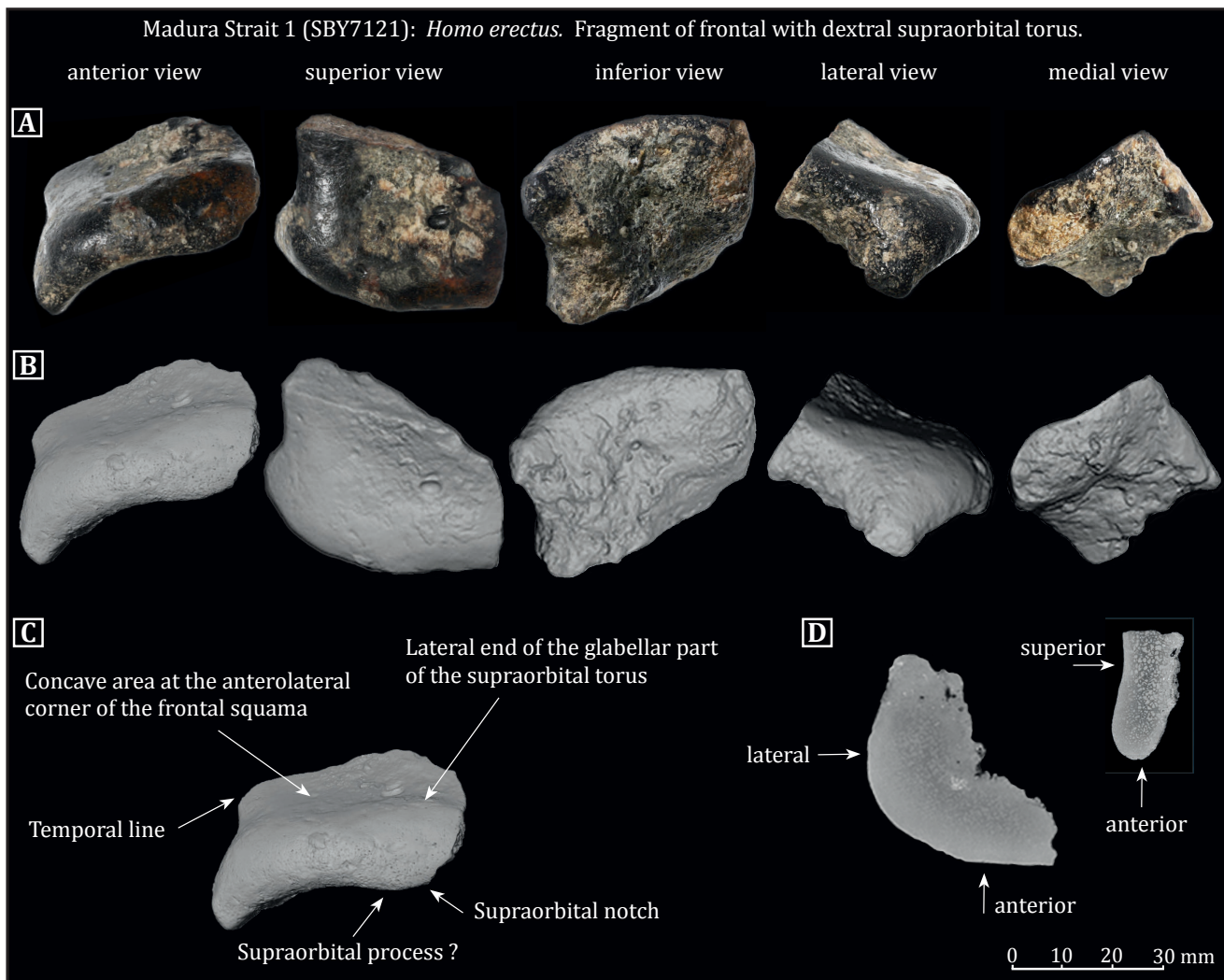


Fig. 4. Madura Strait 1 (MS1): *Homo erectus* frontal fragment with dextral supraorbital torus. **A:** Photographs. **B:** CT-based 3D surface rendered images. Note that the exact orientation of the fragment is unknown. For the anterior view, a slightly diagonal orientation has been assumed. **C:** CT-based 3D surface rendered image of MS1 in a more horizontal orientation, with anatomical indications. **D:** CT-slice.

4.1.2 Madura Strait 2

Madura Strait 2 (Fig. 5) is a right or left parietal fragment with the middle part of the sagittal suture. The preserved linear suture length is 39 mm. The maximum preserved anteroposterior length of the specimen is 45 mm and the maximum preserved mediolateral width is 34 mm. The specimen is heavily mineralized, exhibits a dark color, and is free from taphonomic distortion. All bone surfaces are well-preserved.

The preserved suture is moderately serrated on the ectocranial side, but is smooth and straight on the endocranial side, as often seen in the mid-sagittal suture of fossil and extant *Homo*. Granular foveolae (arachnoid fovea) are present as some depressions on the endocranial surface. The cranial thickness is 8.4 mm along the suture and 7.3 mm along the lateral fracture surface. Along this fracture surface, the bone is made up of an outer table of ~2.1 mm, an intermediate diploë layer of ~3.5 mm, and an inner table of ~1.7 mm.

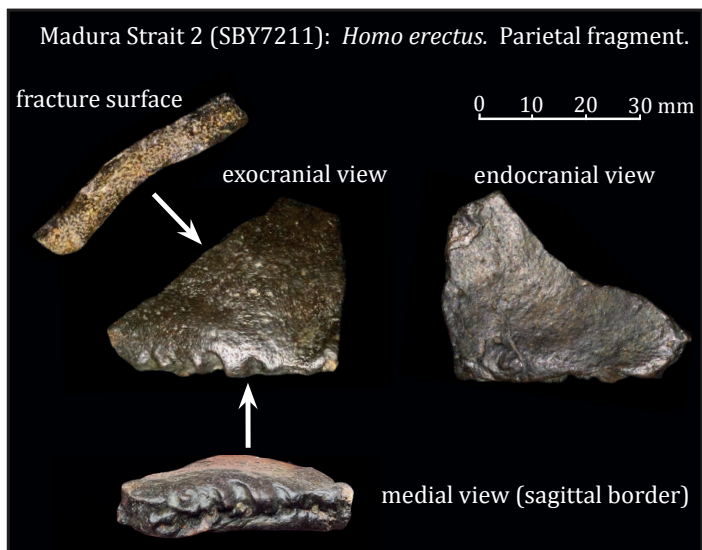


Fig. 5. Madura Strait 2 (MS2): *Homo erectus* parietal fragment with sagittal suture. Photographs. The fragment may either derive from the dextral or sinistral parietal. Orientation (ant-post) of the fragment is unknown.

4.2 Comparisons

4.2.1 Madura Strait 1

Metric comparisons

Table 1 provides metric data of MS1 and crania from the comparative groups. The metric data of comparative skulls derive from previous publications, with the addition of new, unpublished measurements.

In the bivariate plot (**Fig. 6A**) of lateral and midorbit SOT-thicknesses, the late Middle Pleistocene *Homo erectus* from Ngandong stands out by its laterally thickened supraorbital torus, a feature unknown from the earlier *Homo erectus* populations, either from Java or China. The fossils from Sambungmacan and Ngawi exhibit this trend to a lesser extent (together with Ngandong 1). In the late archaic *Homo* from the Asian mainland, the thickness of the supraorbital torus is highly variable. There is some overlap with the Sambungmacan/Ngawi condition, but the lateral thickening such as in the Ngandong crania is absent. MS1 shows a weak lateral thickening of the supraorbital torus, to a condition that is similar to the Sambungmacan/Ngawi crania and Ngandong 1. However, compared to these crania, the torus of MS1 is relatively thin. MS1 also plots relatively close to the Jinnishuan and Xuchang 1 crania, however, as we will see below, these crania strongly differ from MS1 for other metric and morphological aspects.

The bivariate plot of the one-sided postorbital constriction and postorbital breadth (**Fig. 6B**) shows a metric demarcation of the Pleistocene hominin groups from Asia. The early *Homo erectus* from Java and China have a strong postorbital constriction and a relatively small supraorbital breadth, both of which are most pronounced in the late Early Pleistocene crania from Java. The late Middle Pleistocene *Homo erectus* from Java has a low postorbital constriction and modest postorbital breadth. The late Middle Pleistocene late archaic *Homo* crania from northern/central China exhibit a moderate to strong postorbital constriction together with a relatively large postorbital breadth, which reflects the overall large size of these crania.

For the frontal fragment MS1, the full postorbital breadth is unknown. With a preserved postorbital breadth of ~ 40 mm of the right lateral part of the frontal, this value certainly must have exceeded 80 mm. The one-sided postorbital constriction can be measured. Its value, however, depends on the orientation of the frontal fragment, and falls between 5.2 mm (horizontal orientation) and 3.9 mm (diagonal orientation) (**Table 1**). In the bivariate plot of **Fig. 6B**, MS1 again shows a close affinity with the Sambungmacan crania, which are characterized by a very weak postorbital constriction.

Further comparison with the comparative groups from Java

As demonstrated in the above metric comparisons, the late Early Pleistocene *H. erectus* from Java differs from the late Middle Pleistocene *H. erectus* from Java by its strong postorbital constriction and the absence of lateral thickening of the supraorbital torus, although a weak tendency of the latter is observed in Sangiran 17 (Kaifu et al., 2008; Rightmire, 1990; Santa Luca, 1980; Weidenreich, 1951). For both aspects, MS1 is similar to the younger comparative group.

Another difference is that the supraorbital torus of the late Early Pleistocene *H. erectus* from Java is mostly arched around the orbits, whereas the torus of the late Middle Pleistocene *H. erectus* from Java is relatively straight, with a rather flat supratoral plane. Also for this morphological trait, MS1, with its relatively straight supraorbital torus and flat supratoral plane, has a closer affinity with the younger group. Posterior from the supratoral plane, the angle formed with the root of the frontal squama is variable both in the late Early Pleistocene and late Middle Pleistocene groups of Javanese *H. erectus*, ranging from weak posterior (e.g., Sangiran 17, Ngandong 1 and 6) to more vertical (e.g., Skull IX, Ngandong 7 and Sambungmacan 3) inclinations. The preserved root of the frontal squama of MS1 is weakly inclined. However, looking at the anterolateral part of the frontal squama, lateral to the bulging central zone of the frontal squama and medial to the thick temporal line, we note a distinct concavity, which is a trait of the younger comparative group, the late Middle Pleistocene *H. erectus* from Java (**Figs. 4 and 7**).

Thus, MS1 fits comfortably in the comparative group of the late Middle Pleistocene Javanese *H. erectus*. Within this group, the frontal fragment shows a closer affinity with the Sambungmacan crania than with the Ngandong crania, referring to its modest lateral thickening of the supraorbital torus and its weak postorbital constriction. However, the torus of MS1 is thinner than the ten adult and one adolescent individuals in this comparative group (**Fig. 6A, Table 1**). Additionally, the gentle but transversely extensive supraorbital process of MS1 seems to be unique to this specimen (**Fig. 4C**), although the development of this process is variable in the crania from Ngandong, Sambungmacan and Ngawi, from no development to a small but distinct projection (**Fig. 7**). Unfortunately, the frontal bone breadth of

MS1 cannot be estimated with confidence, but the transverse breadth of its preserved part is largely comparable to the equivalent portions of the specimens from this comparative group.

| Specimen | SOTT (mid) | SOTT (lat) | SOTB | POBB | POC 1-sided | data sources |
|-----------------------|---------------|---------------|-------|-------|--------------------------------------|--|
| Madura Strait 1 | 11.5 | 13 | | | 3.9 ^a 5.2 ^b | This study |
| Sangiran 2 | 13 | 12 | 104 | 84 | 10.0 | Kaifu et al. (2008) |
| Sangiran 10 | 14 | | | | | Kaifu et al. (2008) |
| Sangiran 17 | 16 | 16 | 125 | 101 | 12.0 | Kaifu et al. (2008) |
| Bukuran | 14 | 12 | 113 | 88 | 12.5 | Kaifu et al. (2008) |
| Sangiran Skull IX | 13.8 | 12.5 | 111 | 87 | 12.0 | Kaifu et al. (2011a) |
| Sambungmacan 1 | 14 | 16 | 118 | 107 | 5.5 | Kaifu et al. (2008) |
| Sambungmacan 3 | 12 | 15 | 114 | 101 | 6.5 | Kaifu et al. (2008) |
| Sambungmacan 4 | 14 | 16 | 122 | 116 | 3.0 | Kaifu et al. (2008) |
| Ngawi 1 | 13.2 | 15.9 | 114 | 101 | 6.5 | Kaifu et al., 2015 |
| Ngandong 1 (Solo 1) | 12 | 14 | | (106) | (7.0)* | Kaifu et al. (2008); Kaifu, unpublished data |
| Ngandong 5 (Solo 4) | 12 | 16 | 116 | 103 | 6.5 | Kaifu et al. (2008) |
| Ngandong 6 (Solo 5) | 14 | 18 | 122 | 108 | 7.0 | Kaifu et al. (2008) |
| Ngandong 7 (Solo 6) | 12 | 18 | 121 | 106 | 7.5 | Kaifu et al. (2008) |
| Ngandong 10 (Solo 9) | 12 | 18 | 124 | 110 | 7.0 | Kaifu et al. (2008) |
| Ngandong 11 (Solo 10) | 12 | 17 | 132 | 114 | 9.0 | Kaifu et al. (2008) |
| Ngandong 12 (Solo 11) | 13 | 19 | 124 | 107 | 8.5 | Kaifu et al. (2008) |
| Liang Bua 1 | 6.8 | 8 | 88 | 71 | 8.5 | Kaifu et al. (2011b) |
| Zhoukoudian Skull 3 | 10.2 | 9.1 | 108 | 88 | 10.0 | Weidenreich (1943); Kaifu, unpublished data |
| Zhoukoudian Skull 5 | 11.6 | 11.7 | 119 | 96.6 | 11.2 | Kaifu, unpublished data |
| Zhoukoudian Skull 10 | 13.4 | 13.1 | 119 | 98 | 10.5 | Weidenreich (1943); Kaifu, unpublished data |
| Zhoukoudian Skull 11 | 12 | | 113 | 93 | 10.0 | Weidenreich (1943); Kaifu, unpublished data |
| Zhoukoudian Skull 12 | 14.3 | 12.1 | 118 | 95 | 11.5 | Weidenreich (1943); Kaifu, unpublished data |
| Nanjing | 11 | 9 | 107.4 | 90.2 | 8.6 | Kaifu, unpublished data |
| Hexian | 17.2 | 11.8 | 114 | 101 | 6.5 | Kaifu (2017) |
| Dali | 17.1 | 13.6 | 125.5 | 106.4 | 9.6 | Liu et al. (2022); Kaifu, unpublished data |
| Maba | 11.7 | 11.1 | (119) | (102) | (8.5) | Wu and Brauer (1993); Kaifu, unpublished data |
| Harbin | 15 | 15.5 | 145.7 | 125 | 10.4 | Ni et al. (2021); Kaifu and Athreya (in press) |
| Jinniushan | 10.8 | 13.4 | 136.5 | 116 | 10.3 | Ni et al. (2021); Kaifu and Athreya (in press) |
| Xuchang 1 | 9.7 | 12.3 | 143 | 125 | 9.0 | Li et al. (2017); Kaifu and Athreya (in press) |
| Xuchang 4 | 11.7 | | | | | Li et al. (2017) |
| Hualongdong 6 | 16.5 | 11.5 | (124) | 104 | 10.0 | Wu et al. (2021) |
| Narmada | 14.8 | 15.4 | (106) | (94) | 6.0 | Kaifu, unpublished data |

Table 1: Measurements (mm) of the brow region of Madura Strait 1 and comparative Pleistocene crania from Asia. Data in italics are measurements taken from casts. Data in parentheses are estimates.

SOTT = Supraorbital torus thickness, measured at midorbit and the lateral corner.

SOTB = Maximum frontal breadth across the supraorbital tori.

POBB = Least frontal breadth measured posterior to the supraorbital torus.

POC 1-sided = One-sided postorbital constriction = (SOTT-POBB)/2. For MS1, two values are shown. a: specimen in diagonal orientation and b: maximum value with specimen in horizontal orientation.

*: Measured as projected breadth between the landmarks of SOTB and POBB using 3D scan data.

Zhoukoudian 3 and Ngandong 5 are adolescents, all other comparative skulls are adults. Developmental age of MS1 is unknown.

Further comparison with the cranium from Flores

The single existing adult *H. floresiensis* cranium, Liang Bua 1 (LB1), has an arched supraorbital torus (**Fig. 7**) and a relatively strong postorbital constriction (**Fig. 6B**). MS1, with its less arched supraorbital torus and a weaker postorbital constriction, differs from LB1 for both traits. The arched torus and strong postorbital constriction of LB1 resembles more closely the condition of the early Javanese *H. erectus* than the condition of the late Javanese *H. erectus* (Kaifu et al., 2011b).

Most of all, compared to LB1, MS1 has a 60-70% thicker supraorbital torus and a distinctly wider orbit and frontal squama (**Figs. 6 and 7**). Therefore, the diminutive trend that characterizes *H. floresiensis* is absent in MS1.

Further comparison with the comparative groups from the Asian mainland

As shown in the metric comparisons, the brow region of the early Middle Pleistocene northern Chinese *H. erectus* is characterized by an absence of lateral thickening of the supraorbital torus (**Fig. 6A**) and a strong postorbital constriction (**Fig. 6B**). Other relevant traits of this comparative group are an arched supraorbital torus, a distinct supratoral sulcus, as well as a relatively vertical frontal squama with a convex (non-concave) anterolateral surface. For illustrations, see Weidenreich (1943), Viallet et al. (2010), Liu et al. (2014, 2005). MS1 differs from this group in all these aspects.

The frontal bone of the Hexian cranium (see Liu et al. (2014) and Cui and Wu (2015) for illustrations) is similar to MS1 in showing a weak postorbital constriction (**Fig. 6B**). However, it is distinct from MS1 by its supraorbital torus, which is

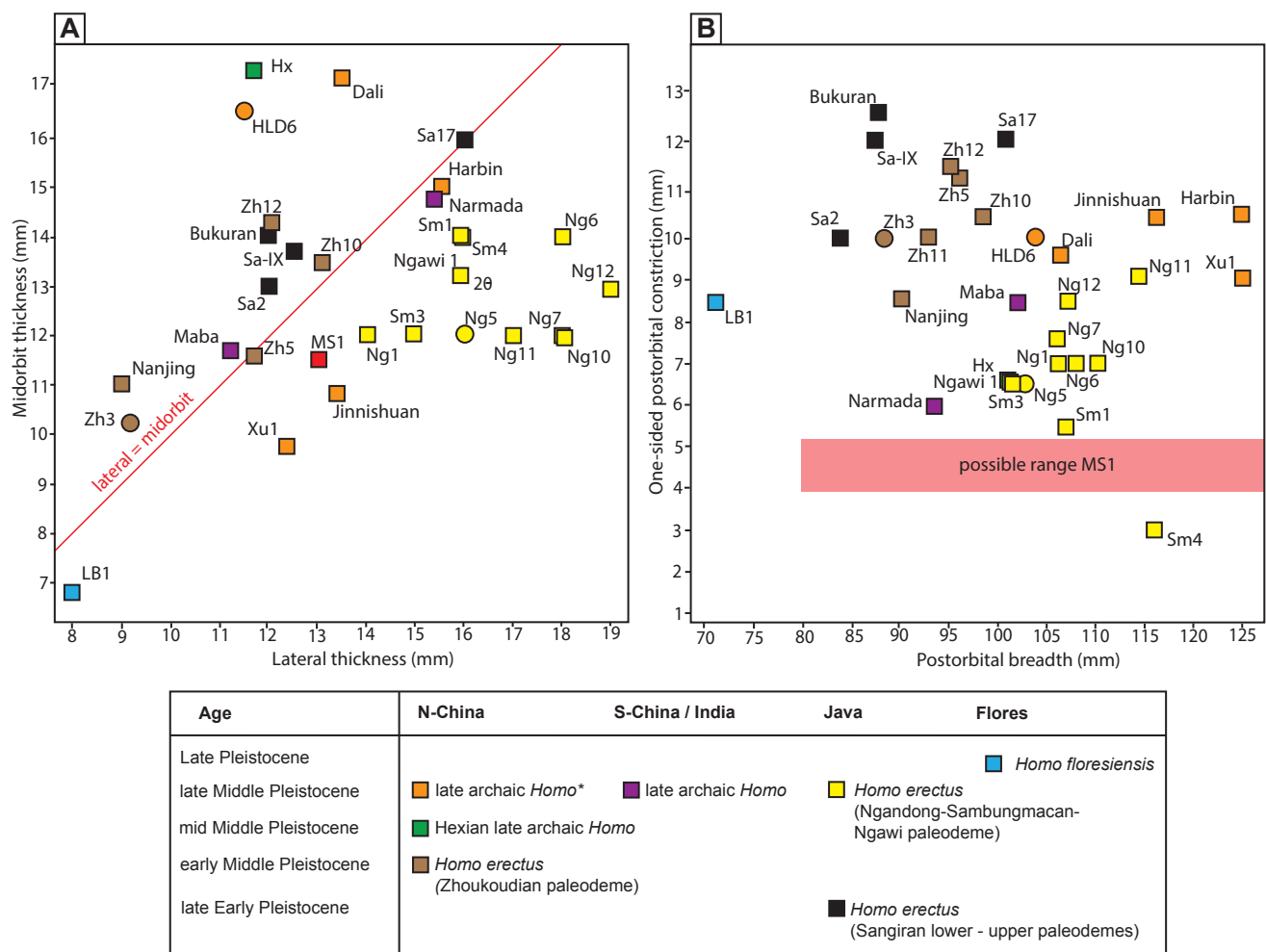


Fig. 6. Bivariate analyses of frontal bone measurements. **A:** Bivariate plot of medial and lateral supraorbital torus thicknesses. **B:** Bivariate plot of one-sided postorbital constriction and postorbital breadth. For details and data sources, see **Table 1**.

*: Xuchang 1 dates from the early Late Pleistocene (Li et al., 2017) or late Middle Pleistocene (Wang et al., 2022).

markedly thickened above the mid-orbit but thin laterally (**Fig. 6A**). Moreover, the supratemporal plane of the Hexian cranium is arched above the orbit and, posterior to this supratemporal plane, its frontal squama stands more vertically.

The late Middle and early Late Pleistocene archaic *Homo* crania from northern/central China form a relevant comparative group, by its age overlap with the Madura Strait specimens. For illustrations of these crania, see Ni et al. (2021), Wu et al. (2021, 2019), Li et al. (2017), Liu et al. (2014), and Wu and Athreya (2013). The thickness of the supraorbital

torus is variable in this group. In Harbin, Hualongdong 6 and Dali, the torus is rather robust, with the latter two having their greatest thickness above the midorbit. The crania from Xuchang and Jinnishuan have more gracile supraorbital tori with a slight lateral thickening, a condition comparable to MS1 (**Fig. 6A**). However, all crania from this group exhibit a moderate degree of postorbital constriction, which contrasts with the very weak constriction in MS1 (**Fig. 6B**). Many of the Chinese crania also have very high postorbital breadths, an aspect that unfortunately cannot be compared with the frontal fragment MS1 (**Fig. 6B**). The late Middle and early Late Pleistocene archaic *Homo* crania from northern/central China are further characterized by a more arched supraorbital torus and a moderately inclined foot of the frontal squama, with a laterally sloping, convex (non-concave) anterolateral part. MS1 differs from these crania for both traits.

The crania from Maba and Narmada (see Liu et al. (2014) and Sonakia (1984) for illustrations) have a variable morphology of the supraorbital torus. Maba does not show a lateral thickening of the torus and exhibits a rather strong postorbital constriction (Wu and Bräuer, 1993). Narmada resembles MS1, in showing a slight lateral thickening of its supraorbital torus, but the entire torus is more robust in Narmada. (**Fig. 6A**). It also resembles MS1 by its weak postorbital constriction (**Fig. 6B**). However, both crania differ from MS1 by their arched supraorbital torus and a more vertically oriented frontal squama, with a convex anterolateral part.

The frontal sinus

There is substantial variation in the size and shape of frontal sinuses in fossil and extant hominins (Balzeau et al.,

2022). In general, sinuses appear to be relatively large in the Early Pleistocene *H. erectus* from Java. The late Middle Pleistocene *H. erectus* from Java, represented by the crania from Ngandong and Sambungmacan, tend to have small, centrally restricted frontal sinuses. In this respect, the absence of a frontal sinus in the preserved part of MS1 (Fig. 4D) matches with this comparative group.

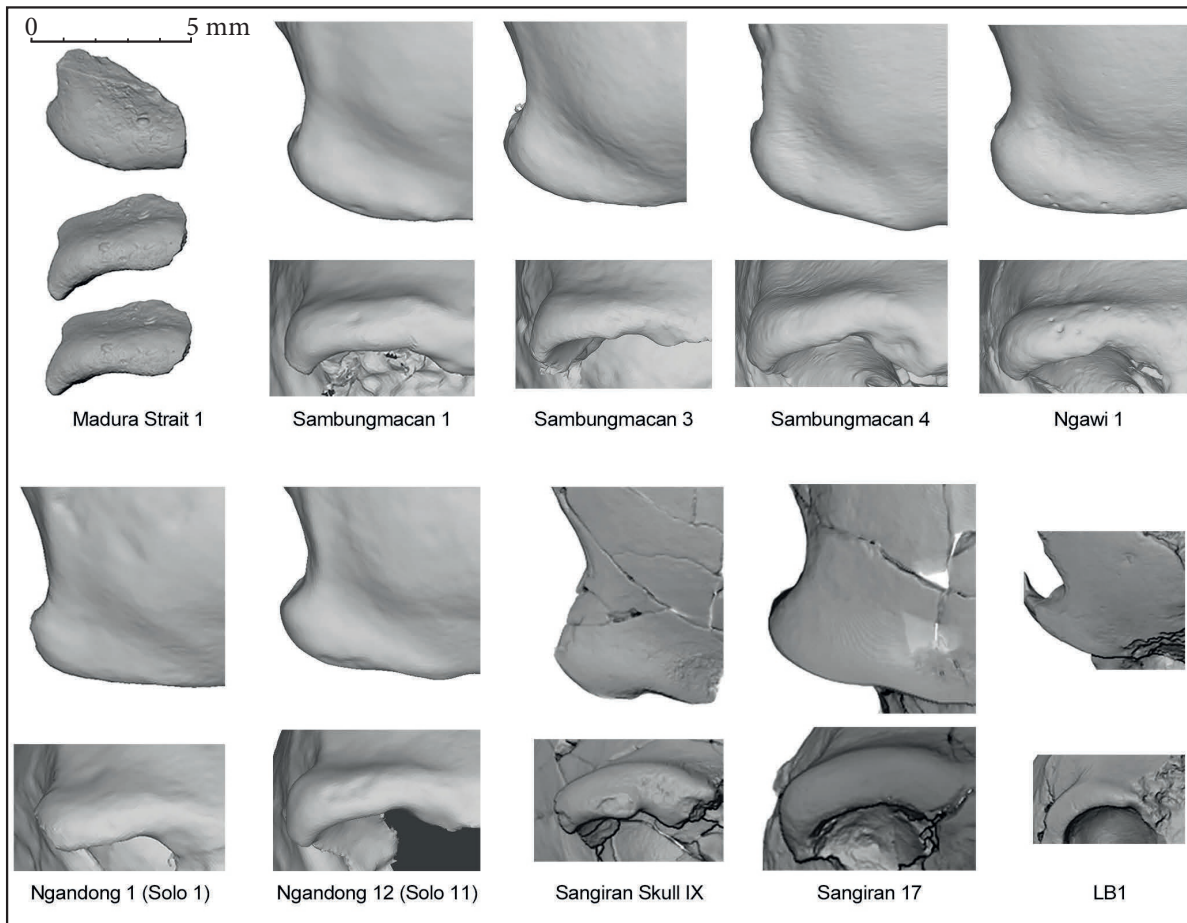


Fig. 7. Frontal and superior views of selected frontal bones from Indonesia. Data obtained from 3D surface scans and CT scans. Two versions of orientation are indicated for the anterior view of MS1 (the upper with reference to Sambungmacan 4 and the lower with reference to Sambungmacan 1, with the superior view based on the former). The left frontals (Sambungmacan 3 and 4) are flipped for ease of comparison.

4.2.1 Madura Strait 2

As a mid-parietal fragment, MS2 lacks the strong sagittal flexion as seen in *Homo sapiens* and may in this respect be regarded as morphologically archaic. The specimen is undiagnostic otherwise. The measured vault thickness along this part of the parietal line falls in the lower range of adult *Homo erectus* as well as modern *Homo sapiens* crania (Balzeau, 2006). The open suture and the modest cranial thicknesses indicate that the specimen derives from an individual that had not reached adulthood at the time of death.

5. Discussion and conclusions

Developmental age

The frontal fragment MS1 has a prominent supraorbital torus and an anteroposteriorly wide supratemporal plane, but the torus thickness is slightly below the range of the known adult crania from Java (Fig. 6A). This suggests that MS1 derives from a gracile adult or otherwise from an adolescent. The specimen does not preserve sutures that could have been indicative for developmental age. However, the available adolescent crania in our comparative sample, i.e. Ngandong 5 and Zhoukoudian 3, indicate that except for a slightly smaller size, their morphological differences from adult individuals from the same paleodeme are limited. Therefore, the uncertain developmental age of MS1 probably has limited impact on our morphological interpretations. The open sutures in the parietal fragment MS2 indicate that this specimen derived from a subadult individual.

Geography and chronology

The two hominin cranial specimens derive from the MIS6 (late Middle Pleistocene) valley fill of the Solo, which makes them contemporaneous to the late Javanese *H. erectus*, also referred to as the Ngandong/Sambungmacan/Ngawi pa-

leodeme. All of the reported fossils from this hominin group derive from the Solo Valley, ca. 150 to 200 km upstream of the Madura Strait subsea site. Therefore, in terms of geography and chronology, the two fossils from the Madura Strait may be tied to the Ngandong-Sambungmacan-Ngawi paleodeme.

Taxonomic affinities

Our comparison with various Asian archaic *Homo* crania indicates that the morphology of the frontal fragment MS1 fits comfortably with the sample of the late Javanese *Homo erectus* (the Ngandong/Sambungmacan/Ngawi paleodeme). It exhibits characteristic features of this group, such as a relatively straight supraorbital torus, a flat supratoral plane, a weak postorbital constriction, and a concave anterolateral portion of the frontal squama that slopes gently posteriorly. Within this sample, MS1 is most similar to the Sambungmacan crania, showing a very weak postorbital constriction and modest lateral thickening of the supraorbital torus.

However, MS1 is somewhat unique compared to our sample of the Ngandong/Sambungmacan/Ngawi paleodeme, in displaying a relatively thin supraorbital torus and a considerable supraorbital process. The limited thickness of the supraorbital torus may reflect a not fully matured individual. However, it is also possible that MS1 was an adult individual, in which case the specimen slightly expands the range of variation of supraorbital torus morphology and thickness of this hominin group. MS2, presumably from a subadult individual, shows an archaic character of modest curvature but is otherwise undiagnostic.

Fig. 8 shows MS1 in direct comparison with Sambungmacan 3, the late Middle Pleistocene *H. erectus* cranium from Java that is metrically close to MS1. In this comparative cranium, the supraorbital plane has a rather horizontal orientation. The original orientation of MS1 is unknown.

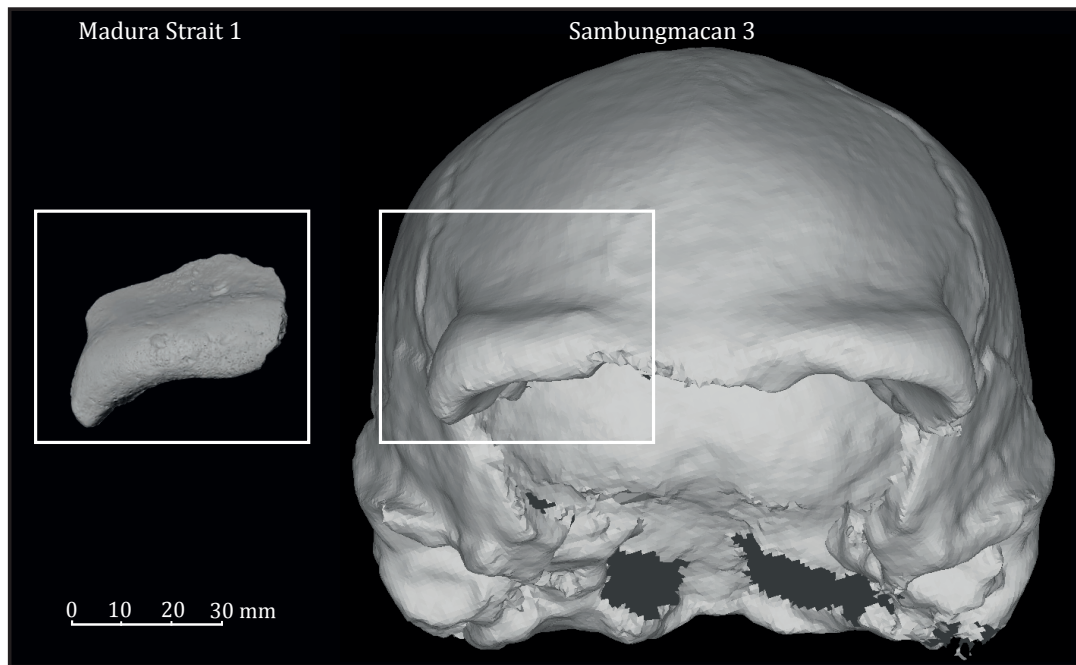


Fig. 8. 3D surface images of MS1 and Sambungmacan 3 (anterior view). This comparative skull has the closest metric and morphological match with MS1.

The MIS6 population of the Solo Valley

The late Javanese *Homo erectus* may be regarded as an MIS6 population living along the banks of the Solo or in the wider catchment area of the Solo. In the Middle Pleistocene climate of Java, characterized by long dry seasons, large perennial rivers such as the Solo probably offered 'fortunate conditions' (Dennell, 2008) for hominin populations, providing drinking water and aquatic food resources and attracting large herbivores. During the MIS6 glacial conditions, the Solo River proceeded eastwards over the exposed shelf of the present-day Madura Strait (Berghuis et al., 2025a, 2022, 2021).

The Madura Strait skull fragments show that the MIS6 *Homo erectus* that we know from Java also dispersed over the surrounding lowland plains, possibly following the course of the Solo. Other groups may very well have populated different areas, following the banks of other lowland rivers on the exposed Sunda Shelf. This lowland habitat places the assumed isolation of the Javanese *Homo erectus* lineage in a different perspective. At least during MIS6, the geographic range of the species exceeded Java and covered a larger area of Sundaland.

The rich vertebrate assemblage from the Madura Strait shows that the same accounted for most other mammalian species that we know from the Javanese fossil localities. This is also in line with the community structure reflected by the Middle Pleistocene vertebrate assemblages from Java, which represent balanced continental conditions, lack evidence of endemism and record the occasional arrival of new herbivore species such as *Elephas hysudrindicus*, *Rusa* sp., and *Axis javanicus*.

Subsea zooarchaeology

If *Homo erectus* and other Middle Pleistocene vertebrate species were able to disperse over the lowland plains of this part of Sundaland, why wouldn't contemporaneous hominin populations from the Asian mainland have been able to do the same, dispersing southwards over this landmass? Moreover, genomic studies on extant human populations have suggested the existence of Denisovans, a non-*erectus* group of archaic *Homo*, in the Sundaland region in the Late Pleistocene, prior to the arrival of anatomically modern humans (Teixeira et al., 2021; Jacobs et al., 2019; Cooper and Stringer, 2013). This also points to southward migration of post-*erectus* populations, from the mainland to Sundaland, but where is the fossil evidence?

Madura Strait 1, with its morphological and metric affinity with the late *Homo erectus* of Java, does not provide an answer to these questions. However, the two skull fragments do underline the potential of subsea hominin localities on the Sunda Shelf. The answers may very well be at the bottom of the sea.

